

## Time-resolved luminescence studies in an $n$ -type $\text{Zn}_{1-x}\text{Cd}_x\text{Se}/\text{ZnS}_y\text{Se}_{1-y}$ quantum well

K. Nakano, Y. Kishita, S. Itoh, M. Ikeda, and A. Ishibashi

*Sony Corporation Research Center, 174 Fujitsuka-cho, Hodogaya-ku, Yokohama 240, Japan*

U. Strauss

*Max-Planck-Institut für Festkörperforschung, Heisenbergstrasse 1, 70506 Stuttgart, Germany*

(Received 10 April 1995; revised manuscript received 23 October 1995)

The recombination processes in an  $n$ -type  $\text{Zn}_{1-x}\text{Cd}_x\text{Se}/\text{ZnS}_y\text{Se}_{1-y}$  quantum well are investigated by time-resolved photoluminescence measurements. The combined analysis of the luminescence decay time and intensity yields the temperature dependence of the radiative and nonradiative recombination time. The quantum efficiency at a low temperature of 8 K is close to unity and the nonradiative recombination rate increases as the temperature is raised. The large effective radiative recombination coefficient of  $1.4 \times 10^{-9} \text{ cm}^3/\text{s}$  at 300 K is attributed to excitonic enhancement, even at 300 K.

### I. INTRODUCTION

ZnSe-based alloys are important materials for the fabrication of blue and green laser diodes. Recently, room-temperature (RT) continuous-wave operation of blue-green and blue lasers has been achieved, using a  $\text{Zn}_{1-x}\text{Cd}_x\text{Se}/\text{ZnS}_y\text{Se}_{1-y}/\text{Zn}_z\text{Mg}_{1-z}\text{S}_y'\text{Se}_{1-y}'$  single-quantum-well separate-confinement heterostructure.<sup>1,2</sup> Since the performance of quantum-well (QW) lasers is governed by the radiative recombination process of carriers in quantum well structures, a detailed study of such a process is highly desirable. Excitons play a major role in the optical properties of QW's especially at low temperatures because of the increase of exciton binding energy and oscillator strength due to size quantization. For III-V QW's, the recombination kinetics of photoexcited carriers, especially in recent years, has been extensively studied both experimentally<sup>3-21</sup> and theoretically.<sup>22-28</sup> Free two-dimensional excitons in smooth interfaces were theoretically predicted to have a long coherence length and an enhanced radiative decay of the order of picoseconds.<sup>23,24</sup> Such short radiative lifetimes have been obtained in a single GaAs QW under resonant excitation.<sup>11</sup> However, a large range of measured decay times (10 ps to 5 ns) were found even in the established GaAs/Al<sub>x</sub>Ga<sub>1-x</sub>As QW system.<sup>7-14</sup> This large scatter is due to the participation of excitons bound to inhomogeneities in the QW structure. These arguments are mainly based on the results of low-temperature experiments. From the application point of view, the optical properties at higher temperature are more important, since RT operation is essential for optoelectronic devices. Recently it has been reported that an important nonradiative mechanism was the thermal emission of the carriers out of the quantum well into the barrier in In<sub>x</sub>Ga<sub>1-x</sub>As/GaAs,<sup>15-19</sup> In<sub>x</sub>Ga<sub>1-x</sub>As/GaAs/Al<sub>y</sub>Ga<sub>1-y</sub>As,<sup>20</sup> and Ga<sub>x</sub>In<sub>1-x</sub>P/Al<sub>y</sub>Ga<sub>z</sub>In<sub>1-y-z</sub>P (Ref. 21) QW's. Thus, in the field of III-V QW's, a comprehensive model of recombination mechanism is being established now.

Since the wide-gap II-VI QW's exhibit significantly larger exciton binding energies, compared to the smaller-band-gap III-V QW structures and it has been discussed that exciton recombination might be important even in RT operation of

laser diodes, many studies have been devoted to the lasing mechanism. Several authors have reported that the optical gain in  $\text{Zn}_{1-x}\text{Cd}_x\text{Se}$  QW lasers arises from a recombination via localized excitonic states.<sup>29-32</sup> On the other hand, a model based on free-carrier transitions was also proposed.<sup>33,34</sup> Furthermore, the very short device lifetime [ $\sim 1$  h at RT (Ref. 35)] means that nonradiative recombination certainly plays a role at RT. Therefore, additional research is required in order to understand the factors that limit the recombination mechanisms in this material and to achieve a clear understanding of the laser characteristics when increasing the temperature up to RT. Time-resolved photoluminescence (PL) spectroscopy is a very powerful technique for the investigation of carrier dynamics in low-dimensional semiconductor structures. To our knowledge, only limited studies<sup>36,37</sup> have reported direct measurements of carrier lifetimes ( $\tau$ ) in this system near RT.

In this paper, we report the direct measurement of  $\tau$  as a function of temperature in  $n$ -type  $\text{Zn}_{1-x}\text{Cd}_x\text{Se}/\text{ZnS}_y\text{Se}_{1-y}$ , which is actually used in laser structures, with time-resolved photoluminescence in the picosecond regime. We determine the radiative and nonradiative lifetimes ( $\tau_r$ ,  $\tau_{nr}$ ), the quantum efficiency ( $\eta$ ), and evaluate the radiative recombination coefficient, which is an important material parameter for light emission and does not depend on material quality, and study the excitonic or band-to-band nature of the radiative recombination in this QW.

### II. EXPERIMENTAL PROCEDURE

The sample used in this work is a  $\text{Zn}_{1-x}\text{Cd}_x\text{Se}/\text{ZnS}_y\text{Se}_{1-y}$  quantum well grown by molecular-beam epitaxy on a (001) GaAs substrate at a temperature of 280 °C. The sample has the following layer sequence: 1  $\mu\text{m}$  of Cl-doped  $\text{ZnS}_{0.07}\text{Se}_{0.93}$  was grown first, followed by 6 nm of Cl-doped  $\text{Zn}_{0.7}\text{Cd}_{0.3}\text{Se}$  and 92 nm of Cl-doped  $\text{ZnS}_{0.07}\text{Se}_{0.93}$ . The confinement energy  $\Delta E$  in the quantum well was 0.30 eV. All three layers were doped under the same conditions. The doping concentration in the  $\text{ZnS}_y\text{Se}_{1-y}$  barriers was  $1.2 \times 10^{17} \text{ cm}^{-3}$ . We supposed that the doping of the  $\text{Zn}_{1-x}\text{Cd}_x\text{Se}$  well is the same.

The sample was optically excited by a 200-fs pulse of a frequency doubled Ti:sapphire laser, synchronously pumped by a mode-locked Ar<sup>+</sup>-ion laser at a repetition rate of 80 MHz. The excitation energy was 3.18 eV. The average power used was typically 20 mW. The laser beam was focused onto the sample to a spot of roughly 50  $\mu\text{m} \times 400 \mu\text{m}$ . However, the laser spot size is insufficient to get a precise value of the carrier density, since we have to take into account the spot profile, reflection at the surface, spectral hole burning, and so on. Therefore, we checked the excitation condition by varying the excitation power. We confirmed that lifetime is independent and the spectral line shape does not broaden with the laser power from 3.5  $\mu\text{W}$  to 30 mW at room temperature and lower temperature. From these observations, we have concluded that generated carrier density by laser pulse is small compared to doping and defect density, respectively.

The photoluminescence was dispersed by a 0.32-m spectrometer and detected by a two-dimensional streak camera with a spectral and temporal resolution of 4 nm and 10 ps, respectively. The experiments were carried out from 8 to 375 K.

### III. RESULTS AND DISCUSSION

The first part of this section contains a theoretical description of the recombination dynamics in large-band-gap II-VI heterostructures. The models of recombination processes in QW's have been developed by several authors.<sup>26-28</sup> We follow these models and write them down for a clarification. Then we present the experimental results and discuss them in detail.

Since  $n$ -type material is investigated in this paper, a high concentration of free carriers is expected in this system. But the presence of excitons up to our highest temperature of 375 K has also to be taken into account, since the exciton binding energy is comparable with thermal energy at 300 K in II-VI heterostructures. As mentioned earlier, it is reasonable for our case to assume the low injection condition for the case of  $n$ -type material (i.e.,  $n_0 \gg \Delta n, \Delta p, p_0$ ), where  $n_0$  ( $p_0$ ) is the equilibrium concentration of majority (minority) carriers and  $\Delta n$  ( $\Delta p$ ) is the excess carrier concentration.

First, we look at a system with only free carriers. The recombination after excitation pulse is described by

$$\frac{d\Delta n_f}{dt} = -Bn_0\Delta n_f - c_f N_J \Delta n_f. \quad (1)$$

The parameters used in the text are defined in Table I. The solutions for  $\Delta n_f(t)$  can be written as

$$\Delta n_f(t) = \Delta n_f(0) \exp(-t/\tau_f), \quad (2)$$

where

$$\frac{1}{\tau_f} = \frac{1}{\tau_{r,f}} + \frac{1}{\tau_{nr,f}}, \quad (3)$$

$$\tau_{r,f} = \frac{1}{Bn_0}, \quad (4)$$

$$\tau_{nr,f} = \frac{1}{c_f N_J}. \quad (5)$$

TABLE I. Symbols used in text.

Symbol	Meaning
$\Delta n_f$	Density of free excess carriers
$\Delta x$	Exciton density
$B$	Coefficient for radiative recombination of free carriers
$B_x$	Coefficient for radiative recombination of excitons
$c_f$	Coefficient describing the capturing at traps for free carriers
$c_x$	Coefficient describing the capturing at traps for excitons
$N_J$	Trap density
$\tau_{r,f} = 1/Bn_0$	Free-carrier radiative lifetime
$\tau_{nr,f} = 1/c_f N_J$	Free-carrier nonradiative lifetime
$\tau_{r,x} = 1/B_x$	Exciton radiative lifetime
$\tau_{nr,x} = 1/c_x N_J$	Exciton nonradiative lifetime
$\tau_r$	Effective radiative lifetime
$\tau_{nr}$	Effective nonradiative lifetime

In a system with only excitons, the rate equation can be written

$$\frac{d\Delta x}{dt} = -B_x \Delta x - c_x N_J \Delta x. \quad (6)$$

Then, a similar solution,

$$\Delta x(t) = \Delta x(0) \exp(-t/\tau_x), \quad (7)$$

is obtained, where

$$\frac{1}{\tau_x} = \frac{1}{\tau_{r,x}} + \frac{1}{\tau_{nr,x}}, \quad (8)$$

$$\tau_{r,x} = \frac{1}{B_x}, \quad (9)$$

$$\tau_{nr,x} = \frac{1}{c_x N_J}. \quad (10)$$

In a system with both excitons and free carriers, the terms of exciton formation and dissociation rates have to be taken into account both in Eq. (1) and Eq. (6). However, these terms can be eliminated by combining Eq. (1) and Eq. (6):

$$\frac{d(\Delta n_f + \Delta x)}{dt} = -Bn_0\Delta n_f - B_x\Delta x - c_f N_J \Delta n_f - c_x N_J \Delta x. \quad (11)$$

We assume quasiequilibrium between excitons and free carriers, since formation and dissociation of excitons are much faster than recombination. Therefore the ratio  $\Delta x/\Delta n_f$  can be described as a function of temperature:

$$\frac{\Delta x}{\Delta n_f} = K(T). \quad (12)$$

Using Eq. (12), Eq. (11) can be rewritten as

$$\frac{d\Delta n_f}{dt} = -B_{\text{eff}}n_0\Delta n_f - c_{\text{eff}}N_J\Delta n_f. \quad (13)$$

We describe effective coefficients for radiative recombination ( $B_{\text{eff}}$ ) and nonradiative recombination ( $c_{\text{eff}}$ ) as

$$B_{\text{eff}} = \frac{B + B_x K(T)/n_0}{1 + K(T)}, \quad (14)$$

$$c_{\text{eff}} = \frac{c_f + c_x K(T)}{1 + K(T)}, \quad (15)$$

respectively. Equation (14) shows that radiative recombination in a system with excitons and free carriers is larger than in a system with only free carriers. The time-dependent carrier density is

$$n(t) = n_0 + \Delta n_f(0)\exp(-t/\tau), \quad (16)$$

with

$$\frac{1}{\tau} = \frac{1}{\tau_r} + \frac{1}{\tau_{\text{nr}}}, \quad (17)$$

$$\tau_r = \frac{1}{B_{\text{eff}}n_0}, \quad (18)$$

$$\tau_{\text{nr}} = \frac{1}{c_{\text{eff}}N_J}. \quad (19)$$

If the excitation pulse is shorter than the lifetime and the exciton formation time is faster than the excitation pulse, the carrier density  $\Delta n_f(0)$  at the end of the excitation pulse is proportional to the excitation power  $P_{\text{ex}}$ .

$$\Delta n_f(0) \sim \frac{P_{\text{ex}}}{1 + K(T)}. \quad (20)$$

It is well known that the luminescence intensity on a short time scale  $I(t)$  is proportional to the radiative recombination rate.<sup>38</sup> So, the total luminescence intensity for both band-to-band and exciton emission is determined by

$$\begin{aligned} I(t) &\sim Bn_0\Delta n_f(t) + B_x\Delta x(t) \\ &= B_{\text{eff}}n_0[1 + K(T)]\Delta n_f(0)\exp(-t/\tau) \\ &= I_0\exp(-t/\tau), \end{aligned} \quad (21)$$

where  $I_0 (=CP_{\text{ex}}/\tau_r)$  is the initial luminescence intensity and  $C$  is a normalization factor, which includes the efficiency of the relaxation processes, from the photoexcited states to the recombination states. We assume that  $C$  does not depend on temperature.

From Eqs. (16) and (21),  $\Delta n_f$  and luminescence intensity decay exponentially, and the initial luminescence intensity  $I_0$  is proportional to  $P_{\text{ex}}$  under our experimental condition ( $\Delta n_f \ll n_0$ ). A set of decay curves from the time-resolved PL measurements are shown in Fig. 1 for different temperatures. Figure 2 shows the dependence of the initial PL intensity on the excitation power. These results are consistent with Eq. (21).

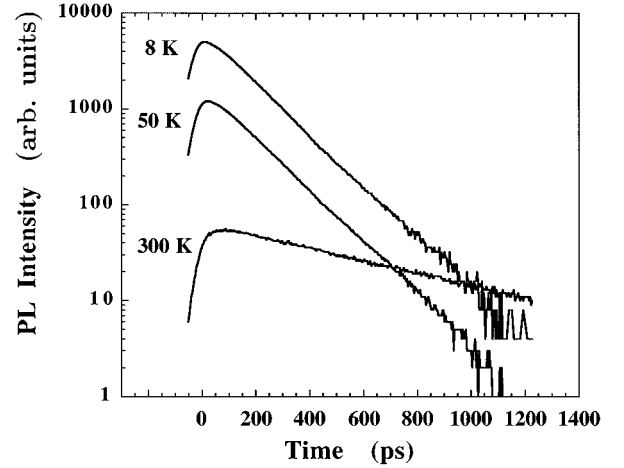


FIG. 1. Typical PL decay curves at three different temperatures on the same scale. The curves are vertically shifted and shown on a logarithmic scale.

The quantum efficiency is expressed in terms of radiative and nonradiative recombination lifetimes. The internal quantum efficiency  $\eta$  can be written as

$$\eta = \frac{1/\tau_r}{1/\tau_r + 1/\tau_{\text{nr}}} = \frac{1/\tau_r}{1/\tau} = \frac{\tau}{\tau_r}. \quad (22)$$

Once we know  $\eta$  at any temperature, we can determine  $CP_{\text{ex}}$  from Eqs. (21) and (22). We can therefore extract both the radiative and nonradiative recombination times for other temperatures, as follows:

$$\tau_r(T) = \frac{CP_{\text{ex}}}{I_0(T)}, \quad (23)$$

$$\tau_{\text{nr}}(T) = \frac{1}{1/\tau(T) - 1/\tau_r(T)}. \quad (24)$$

The two limits of Eq. (22) are case 1,  $K(T) \rightarrow \infty$ , yielding

$$\eta \rightarrow \frac{1/\tau_{r,x}}{1/\tau_{r,x} + 1/\tau_{\text{nr},x}}, \quad (25)$$

and case 2,  $K(T) \rightarrow 0$ , yielding

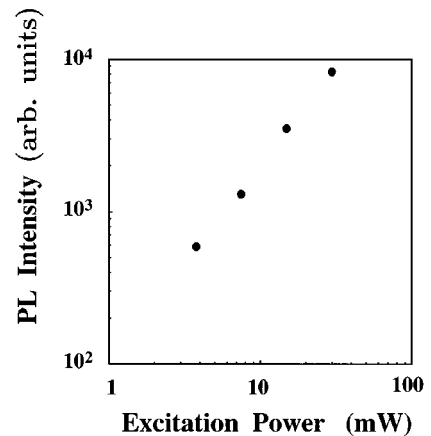


FIG. 2. PL intensity as a function of the excitation power.

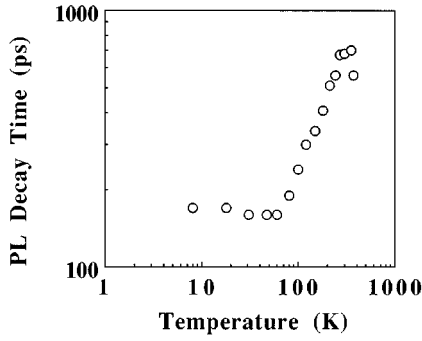


FIG. 3. Temperature dependence of the PL decay time.

$$\eta \rightarrow \frac{1/\tau_{r,f}}{1/\tau_{r,f} + 1/\tau_{nr,f}}. \quad (26)$$

These two cases represent purely excitonic recombination and classical free-carrier recombination, respectively.

Another way to analyze the quantum efficiency is to use the time-integrated PL intensity [ $I_{\text{int}}(T)$ ]. If the time-resolved PL intensity exhibits a monoexponential decay,  $I_{\text{int}}(T)$  is given by

$$I_{\text{int}}(T) = \tau(T)I_0(T) = \frac{\tau(T)CP_{\text{ex}}}{\tau_r(T)} = CP_{\text{ex}}\eta(T). \quad (27)$$

Once we know the value of  $\eta$  at 8 K,  $\eta(T)$  can be estimated by

$$\eta(T) = \frac{I_{\text{int}}(T)}{I_{\text{int}}(8 \text{ K})} \eta(8 \text{ K}). \quad (28)$$

The combined analysis of the PL decay time and intensity is a standard method for determining the recombination time and quantum efficiency.<sup>39</sup> It is worth noting that these relations are correct if it can be assumed that the efficiency of the carrier relaxation processes does not depend on temperature.<sup>10</sup>

Now we present our experimental results. The temperature dependence of the PL decay time is shown in Fig. 3. The change of  $I_{\text{int}}$  with temperature is shown in Fig. 4 (closed circles). At low temperatures ( $T < 60$  K),  $\tau$  and  $I_{\text{int}}$  are almost constant. The drop of the PL intensity at higher temperatures clearly indicates that nonradiative recombination becomes the dominant process.

We now separate the contribution of  $\tau_r$  and  $\tau_{nr}$  from the total lifetime  $\tau$ . We get the relative temperature dependence of  $\tau_r$  from the PL intensity on a ps scale [Eq. (23)]. However, the quantum efficiency for at least one temperature is needed to get the absolute value of  $\tau_r$ . Therefore,  $\tau_r$  is obtained under three assumptions for the quantum efficiency at 8 K:  $\eta(8 \text{ K})=1$ , 0.8, and 0.6. Later it will be shown that  $\eta(8 \text{ K})=1$  is the correct value. We will get  $\tau_{nr}$  from  $\tau$  and  $\tau_r$  with the use of Eq. (24). The data for  $\tau_r$  and  $\tau_{nr}$  are depicted in Fig. 5 and Fig. 6, respectively. Note that the temperature dependence of  $\tau_r$  is similar for all values of  $\eta$ . In contrast, the behavior of  $\tau_{nr}$  is very sensitive to  $\eta$ : we get a *decreasing* nonradiative recombination lifetime with increasing  $T$  if we assume  $\eta(8 \text{ K})=1$ . The values of  $\tau_{nr}(T)$  are *constant* or *increase* with  $T$ , if we assume  $\eta(8 \text{ K})=0.8$  or 0.6, respectively.

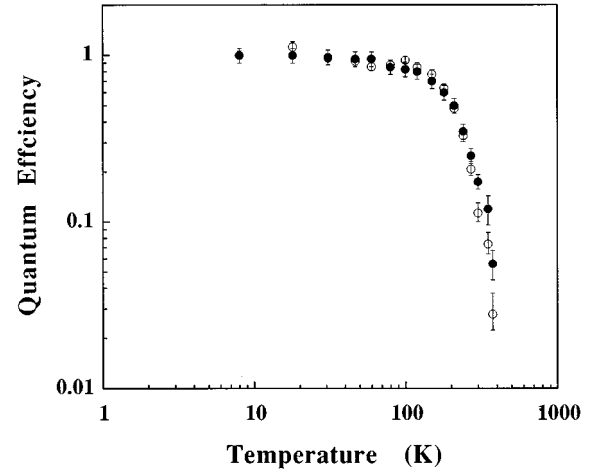


FIG. 4. Quantum efficiency as a function of temperature. Open circles and closed circles are deduced from carrier lifetime [Eq. (22)] and from time-integrated PL intensity [Eq. (28)], respectively.

Due to the small contribution to  $\tau$ , it is not surprising that the values of  $\tau_{nr}$  scatter for  $T < 100$  K.

When determining the temperature dependence of  $\tau_{nr}$ , it is helpful to measure  $\tau$  above 300 K, since the nonradiative process is dominant at high temperature and the temperature dependence of  $\tau$  represents that of  $\tau_{nr}$  itself. As seen in Fig. 3,  $\tau$  decreases with  $T$  at very high temperatures. In general, there are several deep levels in semiconductors. However, it would happen that one kind of deep level whose concentration is high and which has the large capture cross section for minority carriers largely affects the recombination process and only this level affects lifetime explicitly in the temperature range of the measurement. It is thought to be sufficient to assume a single deep level in our sample, since the PL decay curves do not show multicomponent behavior. If there is one predominant nonradiative process, the temperature dependence of  $\tau_{nr}$  for  $T < 300$  K would also show a similar behavior at  $T > 300$  K, i.e., a monotonous decrease, which we get for  $\eta(8 \text{ K})=1$ .

Next we discuss the mechanism of nonradiative recombination. The nonradiative lifetime due to trapping at interface states can be written as

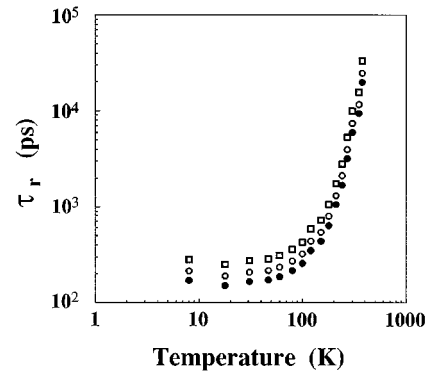


FIG. 5. Temperature dependence of the radiative recombination time. The three different symbols correspond to different assumptions for values of the radiative efficiency at 8 K, namely,  $\eta(8 \text{ K})=1.0$  (closed circles), 0.8 (open circles), and 0.6 (squares). It is shown in the text that  $\eta=1$  is the correct value.

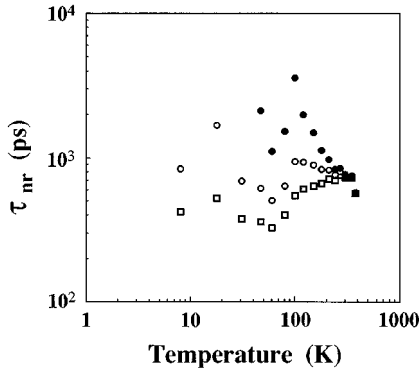


FIG. 6. Temperature dependence of the nonradiative recombination time. The three different symbols correspond to the assumptions of  $\eta(8\text{ K})=1.0$  (closed circles), 0.8 (open circles), and 0.6 (squares). It is shown in the text that  $\eta=1$  is the correct value.

$$\tau_{nr} = \frac{d}{2S} = \frac{d}{\sigma_{\infty} \exp(-E_a/kT) v_{th} N_s}, \quad (29)$$

where  $d$  is the active layer thickness,  $S$  is the interfacial recombination velocity,  $\sigma_{\infty}$  is the capture cross section at an infinite temperature,  $E_a$  is the activation energy,  $v_{th} = \sqrt{3kT/m^*}$  is the thermal velocity ( $m^*$  is the effective mass), and  $N_s$  is the planar density of recombination centers. If nonradiative recombination occurs in the well, we expect the lifetime to vary as

$$\tau_{nr} = \frac{1}{\sigma_{\infty} \exp(-E_a/kT) v_{th} N_T}, \quad (30)$$

where  $N_T$  is the concentration of defect centers. In both cases, we expect the nonradiative process is a thermally activated process. Figure 7 shows the Arrhenius plot of  $\tau_{nr} T^{1/2}$  for the cases of  $\eta(T=8\text{ K})=1.0, 0.8$ . Extracted  $\tau_{nr}$  for  $\eta(T=8\text{ K})=1.0$  gives the best fit to the straight line whose activation energy  $E_a$  is 11 meV.

We now compare our results with previous studies. Two explanations have been proposed for the drop in the PL lifetime at high temperatures in III-V QW's. Pickin and David<sup>26</sup>

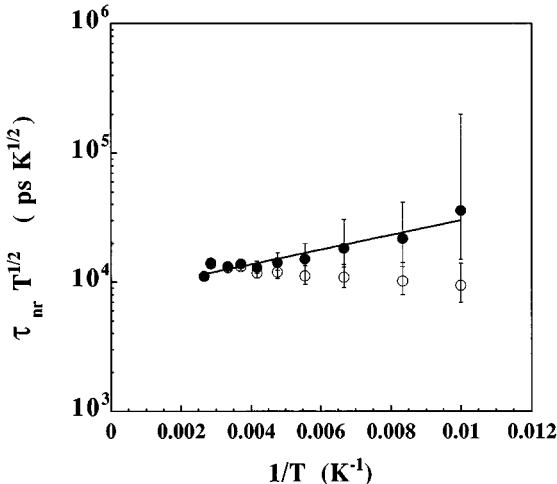


FIG. 7. Arrhenius plot of  $\tau_{nr} T^{1/2}$  for  $\eta(8\text{ K})=1.0$  (closed circles) and 0.8 (open circles), respectively.

concluded that the surface recombination and/or Shockley-Read recombination via interface states are the main nonradiative decay channels in GaAs/Al<sub>x</sub>Ga<sub>1-x</sub>As QW's. Michler *et al.*<sup>21</sup> suggested the importance of thermal emissions of carriers out of Ga<sub>x</sub>In<sub>1-x</sub>P/Al<sub>y</sub>Ga<sub>2</sub>In<sub>1-y-z</sub>P QW's and have shown the activation energy  $E_a$  may be equal to half of the total confinement energy  $\Delta E$  of the electron and hole in the low-injection case. Some reports on Zn<sub>1-x</sub>Cd<sub>x</sub>Se QW's (Refs. 40–42) conclude that the temperature dependence of PL intensity is described by thermal activation of carriers out of the well, since the order of the activation energies is comparable to the barrier heights. However, since our activation energy of nonradiative lifetime is much smaller than  $\Delta E$ , our case should not be attributed to thermal emission out of the well. This thermal emission process from the well might not be the preferable decay channel in our II-VI wells due to the large confinement energy. The considerations above indicate that nonradiative recombination can be described by Shockley-Read-Hall statics and, moreover, that  $\eta$  is 1.0 at 8 K. Just recently Massa *et al.*<sup>43</sup> found three deep levels and observed deep-level luminescence in iodine-doped ZnSe from PL decay measurements. However, we did not see any deep-level luminescence from 500 to 700 nm and the activation energy we deduced does not correspond to any level they observed. This suggests that our sample has a different type of trap.

If we assume a capture cross section ( $\sigma_{\infty}$ ) of  $10^{-14}\text{ cm}^2$ , we can estimate  $N_T$  and  $N_s$  to be  $1.4 \times 10^{16}\text{ cm}^{-3}$  and  $4.3 \times 10^9\text{ cm}^{-2}$ , respectively. From our data, we cannot determine if the process occurs in the bulk or at the interface. A detailed study of the well thickness dependence will allow us to determine which nonradiative recombination mechanism applies.

Next we will discuss the results obtained for  $\tau_r$ . Looking at our results in Fig. 5, it is interesting to note that the radiative lifetimes are nearly independent of temperature at low temperatures ( $T < 60\text{ K}$ ). This behavior might be attributed to the effect of localized excitons with a temperature-independent transition probability,<sup>46</sup> since our sample has a Cl-doped alloy well. As temperature increases, the slope of  $\tau_r$  increases continuously. Hangleiter<sup>25</sup> studied the effect of the Coulomb interaction of electrons and holes in a two-dimensional semiconductor and proposed a model for the temperature dependence of the radiative recombination time in QW. According to this model, we expect  $\tau_r$  to be proportional to  $T$  in quantum wells for only excitons or for only free carriers. In the transition region from a purely excitonic system to only a free carrier system, excitonic bound states become ionized and the radiative lifetime increases rapidly with increasing  $T$ , since free carriers have a longer lifetime than excitons. In this transition temperature range, the slope of  $\tau_r(T)$  is expected to be much larger than unity. As a whole,  $\tau_r$  is expected to show an S-shaped temperature dependence from pure excitonic states to pure free-carrier-like states in the In<sub>x</sub>Ga<sub>1-x</sub>As QW system.<sup>25</sup> However, this is not the case for our sample. The continuous increase of the slope of  $\tau_r$  over 300 K suggests that both excitons and free carriers are present even at 300 K.

Using  $n_0$  of  $1.2 \times 10^{17}\text{ cm}^{-3}$ , we derive a value for the  $B$  coefficient of  $1.4 \times 10^{-9}\text{ cm}^3/\text{s}$  at 300 K. For band-to-band radiative process in Zn<sub>1-x</sub>Cd<sub>x</sub>Se quantum wells, numerical

TABLE II. Parameters used in the calculation.

	Zn <sub>0.7</sub> Cd <sub>0.3</sub> Se
Band gap	2.334 eV <sup>a</sup>
Transition energy	2.41 eV <sup>b</sup>
Spin-orbit splitting	0.43 eV <sup>c</sup>
Effective mass of electron	0.151 $m_0^a$
Effective mass of heavy hole	0.555 $m_0^c$
Effective mass of light hole	0.145 $m_0^c$
Refractive index	3.043 <sup>a</sup>

<sup>a</sup>Reference 44.<sup>b</sup>Measured value.<sup>c</sup>Reference 45.

calculation<sup>5</sup> gives  $B = 1.75 \times 10^{-10} \text{ cm}^3/\text{s}$ . The parameters used in the calculation are listed in Table II. This value is one order of magnitude smaller than our experimental value of  $B_{\text{eff}}$ . This discrepancy can be also interpreted as strong excitonic enhancement of radiative recombination in two-dimensional semiconductors even at room temperature. We expect stronger excitonic enhancement of radiative recombination in our material than in materials with small exciton binding energy such as GaAs or In<sub>x</sub>Ga<sub>1-x</sub>As.

Finally, we compare the results of  $\eta(T)$  from time-integrated PL intensity [Eq. (28)] with the results of  $\eta(T)$  from  $\tau_r$  and  $\tau_{\text{nr}}$  [Eq. (22)]. Both dependences are found to be in good agreement, as shown in Fig. 4. The quantum efficiency  $\eta$  at 300 K is about 14%. Note that this value is extracted in the low excitation regime. The lasing will occur at higher carrier density, which is estimated to be about  $8.3 \times 10^{18} \text{ cm}^{-3}$ .<sup>47</sup> This value is just below the exciton phase-space filling density at which the exciton phase becomes unstable with respect to an electron-hole plasma and which is estimated to be  $1/(\pi a_B^2) \sim 5.7 \times 10^{12} \text{ cm}^{-2}$  ( $a_B$  is the Bohr radius of the excitons in ZnSe), corresponding to  $9.5 \times 10^{18} \text{ cm}^{-3}$  in the 6-nm quantum wells considered here. Furthermore, Hangleiter showed that even at room temperature and for the exciton phase-space filling density, the two-particle correlation effects were expected to be significant even in the In<sub>x</sub>Ga<sub>1-x</sub>As QW system.<sup>25</sup> So excitonic enhancement might still play a role in lasing in II-VI QW lasers even at room temperature, unlike the case of III-V lasers. In the low excitation regime, the quantum efficiency is limited by the com-

petition between the monomolecular radiative and nonradiative recombination process, while the bimolecular radiative process will overcome the monomolecular process in the high excitation regime. Then the quantum efficiency approaches unity. At the threshold carrier density for lasing, the quantum efficiency is estimated to be 90%. About a 10% increase in threshold current is expected compared to the ideal material.

#### IV. CONCLUSION

We have studied the recombination mechanisms of the *n*-type Zn<sub>1-x</sub>Cd<sub>x</sub>Se/ZnS<sub>y</sub>Se<sub>1-y</sub> quantum well by time-resolved photoluminescence measurements. The strong temperature dependence of the PL decay time and intensity were observed. Using these data, the temperature dependence of  $\tau_r(T)$  and  $\tau_{\text{nr}}(T)$  is determined in the Zn<sub>1-x</sub>Cd<sub>x</sub>Se QW system. These results suggest that excitonic radiative recombination governs the carrier decay at low temperatures (<60 K) and the quantum efficiency at a low temperature of 8 K is close to unity. Nonradiative recombination processes become dominant as the temperature is raised. Thermally activated nonradiative recombination processes reduce the luminescence quantum efficiency to 14% at 300 K. This value of  $\eta$  indicates that the quality of the active region of the II-VI laser could be improved further. Furthermore, the low activation energy of the nonradiative channel suggests that the thermal emission out of the well into the barrier is less important in our sample, unlike previous reports.<sup>40-42</sup> From the device point of view, this result is favorable since it demonstrates that the reduction of the quantum efficiency due to the thermal emission can be avoided by employing the large confinement energy. The effective radiative recombination coefficient, which is an important material parameter for device modeling and device improvement, is determined as  $1.4 \times 10^{-9} \text{ cm}^3/\text{s}$  at 300 K. We would like to emphasize that the strong radiative recombination rate in a Zn<sub>1-x</sub>Cd<sub>x</sub>Se quantum-well system is attributed to excitonic enhancement, even at 300 K. High radiative recombination at 300 K is preferable for high efficiency of light-emitting devices.

#### ACKNOWLEDGMENTS

The authors thank Professor H. J. Queisser and W. W. Rühle for many valuable discussions.

- <sup>1</sup>N. Nakayama, S. Itoh, T. Ohata, K. Nakano, H. Okuyama, M. Ozawa, A. Ishibashi, M. Ikeda, and Y. Mori, *Electron. Lett.* **29**, 1488 (1993).
- <sup>2</sup>N. Nakayama, S. Itoh, H. Okuyama, M. Ozawa, T. Ohata, K. Nakano, M. Ikeda, A. Ishibashi, and Y. Mori, *Electron. Lett.* **29**, 2194 (1993).
- <sup>3</sup>G. W. 't Hooft, M. R. Leys, and H. J. Talen-v.d. Mheen, *Superlatt. Microstruct.* **1**, 307 (1985).
- <sup>4</sup>J. E. Fouquet and A. E. Siegman, *Appl. Phys. Lett.* **46**, 280 (1985).
- <sup>5</sup>D. Bimberg, J. Christen, A. Werner, M. Kunst, G. Weimann, and W. Schlapp, *Appl. Phys. Lett.* **49**, 76 (1986).
- <sup>6</sup>J. P. Bergman, P. O. Holtz, B. Monemar, M. Sundaram, J. L.

Merz, and A. C. Gossard, *Phys. Rev. B* **43**, 4765 (1991).

- <sup>7</sup>J. Christen, D. Bimberg, A. Steckenborn, and G. Weimann, *Appl. Phys. Lett.* **44**, 84 (1984).
- <sup>8</sup>J. Feldmann, G. Peter, E. O. Göbel, P. Dawson, K. Moore, C. Foxon, and R. J. Elliott, *Phys. Rev. Lett.* **59**, 2337 (1987).
- <sup>9</sup>P. Zhou, H. X. Jiang, R. Bannwart, S. A. Solin, and G. Bai, *Phys. Rev. B* **40**, 11 862 (1989).
- <sup>10</sup>M. Gurioli, A. Vinattieri, M. Colocci, C. Deparis, J. Massies, G. Neu, A. Bosacchi, and S. Franchi, *Phys. Rev. B* **44**, 3115 (1991).
- <sup>11</sup>B. Deveaud, F. Clérot, N. Roy, K. Satzke, B. Sermage, and D. S. Katzer, *Phys. Rev. Lett.* **67**, 2355 (1991).
- <sup>12</sup>Ph. Roussignol, C. Delalande, A. Vinattieri, L. Carraresi, and M. Colocci, *Phys. Rev. B* **45**, 6965 (1992).

- <sup>13</sup>V. Srinivas, J. Hryniewicz, Y. J. Chen, and C. E. C. Wood, *Phys. Rev. B* **46**, 10 193 (1992).
- <sup>14</sup>J. Martinez-Pastor, A. Vinattieri, L. Carraresi, M. Colocci, Ph. Roussignol, and G. Weimann, *Phys. Rev. B* **47**, 10 456 (1993).
- <sup>15</sup>J. D. Lambkin, D. J. Dunstan, K. P. Homewood, L. K. Howard, and M. T. Emeny, *Appl. Phys. Lett.* **57**, 1986 (1990).
- <sup>16</sup>G. Bacher, H. Schweizer, J. Kovac, A. Forchel, H. Nickel, W. Schlapp, and R. Lösch, *Phys. Rev. B* **43**, 9312 (1991).
- <sup>17</sup>M. Gurioli, J. Martinez-Pastor, M. Colocci, C. Deparis, B. Chastaingt, and J. Massies, *Phys. Rev. B* **46**, 6922 (1992).
- <sup>18</sup>G. Bacher, C. Hartmann, H. Schweizer, T. Held, G. Mahler, and H. Nickel, *Phys. Rev. B* **47**, 9545 (1993).
- <sup>19</sup>J. R. Botha and A. W. R. Leitch, *Phys. Rev. B* **50**, 18 147 (1994).
- <sup>20</sup>M. Vening, D. J. Dunstan, and K. P. Homewood, *Phys. Rev. B* **48**, 2412 (1993).
- <sup>21</sup>P. Michler, A. Hangleiter, M. Moser, M. Geiger, and F. Scholz, *Phys. Rev. B* **46**, 7280 (1992).
- <sup>22</sup>Y. Arakawa, H. Sakaki, M. Nishioka, J. Yoshino, and T. Kamiya, *Appl. Phys. Lett.* **46**, 519 (1985).
- <sup>23</sup>E. Hanamura, *Phys. Rev. B* **38**, 1228 (1988).
- <sup>24</sup>L. C. Andreani, F. Tassone, and F. Bassani, *Solid State Commun.* **77**, 641 (1991).
- <sup>25</sup>A. Hangleiter, *Phys. Rev. B* **48**, 9146 (1993).
- <sup>26</sup>W. Pickin and J. P. R. David, *Appl. Phys. Lett.* **56**, 268 (1990).
- <sup>27</sup>B. K. Ridley, *Phys. Rev. B* **41**, 12 190 (1990).
- <sup>28</sup>O. Brandt, K. Kanamoto, M. Gotoda, T. Isu, and N. Tsukada, *Phys. Rev. B* **51**, 7029 (1995).
- <sup>29</sup>J. Ding, H. Jeon, T. Ishihara, M. Hagerott, A. V. Nurmikko, H. Luo, N. Samarth, and J. Furdyna, *Phys. Rev. Lett.* **69**, 1707 (1992).
- <sup>30</sup>J. Ding, M. Hagerott, T. Ishihara, H. Jeon, and A. V. Nurmikko, *Phys. Rev. B* **47**, 10 528 (1993).
- <sup>31</sup>J. Ding, M. Hagerott, P. Kelkar, A. V. Nurmikko, D. C. Grillo, L. He, J. Han, and R. L. Gunshor, *Phys. Rev. B* **50**, 5787 (1994).
- <sup>32</sup>Y. Kawakami, I. Hauksson, H. Stewart, J. Simpson, I. Galbraith, K. A. Prior, and B. C. Cavenett, *Phys. Rev. B* **48**, 11 994 (1993).
- <sup>33</sup>P. M. Mensz, *J. Cryst. Growth* **138**, 697 (1994).
- <sup>34</sup>R. Cingolani, R. Rinaldi, L. Calcagnile, P. Prete, P. Sciacovelli, L. Tapfer, L. Vanzetti, G. Mula, F. Bassani, L. Sorba, and A. Franciosi, *Phys. Rev. B* **49**, 16 769 (1994).
- <sup>35</sup>A. Ishibashi, *IEEE J. Select. Top. Quantum Electron.* **1**, 741 (1995).
- <sup>36</sup>J. Ding, M. Hagerott, P. Kelkar, A. V. Nurmikko, D. C. Grillo, Li He, J. Han, and R. L. Gunshor, *J. Cryst. Growth* **138**, 719 (1994).
- <sup>37</sup>J. S. Massa, G. S. Buller, A. C. Walker, G. Horsburgh, J. T. Mullins, K. A. Prior, and B. C. Cavenett, *Appl. Phys. Lett.* **66**, 1346 (1995).
- <sup>38</sup>W. van Roosbroeck and W. Shockley, *Phys. Rev.* **94**, 1558 (1954).
- <sup>39</sup>R. C. Miller, D. A. Kleinman, W. A. Nordland, Jr., and A. C. Gossard, *Phys. Rev. B* **22**, 863 (1980).
- <sup>40</sup>C. T. Walker, J. M. DePuydt, M. A. Haase, J. Qiu, and H. Cheng, *Physica* **185B**, 27 (1993).
- <sup>41</sup>Z. Zhu, H. Yoshihara, K. Takebayashi, and T. Yao, *Appl. Phys. Lett.* **63**, 1678 (1993).
- <sup>42</sup>E. Tournié, C. Morhain, M. Leroux, C. Ongaretto, and J. P. Faure, *Appl. Phys. Lett.* **67**, 103 (1995).
- <sup>43</sup>J. S. Massa, G. S. Buller, A. C. Walker, J. Simpson, K. A. Prior, and B. C. Cavenett, *Appl. Phys. Lett.* **67**, 61 (1995).
- <sup>44</sup>Yi-hong Wu, *IEEE J. Quantum Electron.* **30**, 1562 (1994).
- <sup>45</sup>R. Cingolani, P. Prete, D. Greco, P. V. Giugno, M. Lomascolo, R. Rinaldi, L. Calcagnile, L. Vanzetti, L. Sorba, and A. Franciosi, *Phys. Rev. B* **51**, 5176 (1995).
- <sup>46</sup>G. Bacher, J. Kovac, K. Streubel, H. Schweizer, and F. Scholz, *Phys. Rev. B* **45**, 9136 (1992).
- <sup>47</sup>P. Rees, F. P. Logue, J. F. Donegan, J. F. Heffernan, C. Jordan, and J. Hegarty, *Appl. Phys. Lett.* **67**, 3780 (1995).